

# Linking drought indices in the Atlantic sector of the High Arctic (Svalbard) to atmospheric circulation

Krzysztof Migala<sup>1</sup>, Ewa Lupikasza<sup>2</sup>, Marzena Osuch<sup>3</sup>, Magdalena Opała-Owczarek<sup>4</sup>, and Piotr Owczarek<sup>5</sup>

<sup>1</sup>University of wrocław

<sup>2</sup>University of Silesia in Katowice

<sup>3</sup>Polish Academy of Sciences

<sup>4</sup>University of Silesia

<sup>5</sup>Uniwersity of wrocław

December 7, 2022

## Abstract

Based on the long-term climatological data from Ny Alesund, Svalbard Airport – Longyearbyen and Hornsund Polish Polar Station, we undertook an analysis of drought indices on West Spitsbergen Island, Svalbard for the period 1979-2019.

The features and causes of spatio-temporal variability of atmospheric drought on Svalbard were identified, as expressed by the Standardised Precipitation Evapotranspiration Index (SPEI).

It was possible to indicate several-years long periods with the SPEI indicating a domination of drought or wet conditions. Long-term variability of annual and half-year (May-October) values of SPEI showed a prevalence of droughts in the 80-ties and in the first decade of the 21<sup>st</sup> century while wet seasons were frequent in the 90-ties and in the second decade of the 21<sup>st</sup> century. Seasonal SPEIs were characteristic of great inter-annual variability. In MAM and JJA droughts were more frequent after 2000; in the same period in SON and DJF, the frequency of wet seasons increased. The most remarkable changes in the scale of the entire research period were estimated for autumn where negative values of SPEI occur more often in the first part of the period and positive values dominate in the last 20 years.

The long-term course of the variables in subsequent seasons between 1979-2019 indicates strong relationships between the SPEI drought index and anomalies of precipitable water and somewhat weaker relationships with anomalies of sea level pressure.



## 18 **Abstract**

19 Based on the long-term climatological data from Ny Alesund, Svalbard Airport – Longyearbyen  
20 and Hornsund Polish Polar Station, we undertook an analysis of drought indices on West  
21 Spitsbergen Island, Svalbard for the period 1979-2019.

22 The features and causes of spatio-temporal variability of atmospheric drought on Svalbard were  
23 identified, as expressed by the Standardised Precipitation Evapotranspiration Index (SPEI).

24 It was possible to indicate several-years long periods with the SPEI indicating a domination of  
25 drought or wet conditions. Long-term variability of annual and half-year (May-October) values of  
26 SPEI showed a prevalence of droughts in the 80-ties and in the first decade of the 21<sup>st</sup> century  
27 while wet seasons were frequent in the 90-ties and in the second decade of the 21<sup>st</sup> century.  
28 Seasonal SPEIs were characteristic of great inter-annual variability. In MAM and JJA droughts  
29 were more frequent after 2000; in the same period in SON and DJF, the frequency of wet seasons  
30 increased. The most remarkable changes in the scale of the entire research period were estimated  
31 for autumn where negative values of SPEI occur more often in the first part of the period and  
32 positive values dominate in the last 20 years.

33 The long-term course of the variables in subsequent seasons between 1979-2019 indicates strong  
34 relationships between the SPEI drought index and anomalies of precipitable water and somewhat  
35 weaker relationships with anomalies of sea level pressure.

36 **Keywords:** Drought index, atmospheric circulation, SPEI, Svalbard, Arctic.

## 37 **1 Introduction**

38 Feedback mechanisms cause an Arctic amplification manifesting itself as an unprecedented  
39 increase in air temperature and liquid precipitation totals in polar regions as compared with  
40 temperate and tropical latitudes (Pithan and Mauritsen, 2014, IPCC 2019, Łupikasza et al. 2019a).  
41 These changes will likely continue in the future increasing both air temperatures and precipitation  
42 amount (IPCC 2021, Liu et al., 2021), facilitating changes in weather and climate-based drivers of  
43 glacier recession and thinning (van Pelt et al., 2019, Noel et al., 2020), permafrost degradation and  
44 defragmentation (Schaefer et al., 2014, Biskaborn et al., 2019, Strand et al., 2021), and increasing  
45 ecological risk for the whole ecosystem (Hinzman et al., 2013, Anderson et al., 2017, Owczarek  
46 et al., 2021).

47 The frequency and range of extreme climate events are thought to be the significant drivers  
48 of environmental changes (Walsh et al. 2020). The extreme events in the Arctic, such as  
49 abnormally dry conditions (drought) and heavy precipitation also significantly influence the fragile  
50 polar ecosystems. However, their environmental effects in warm/vegetation season are different  
51 from those in winter season.

52 Zang et al. (2020) studied variations of drought during the vegetation seasons in Northern  
53 Hemisphere and found that the duration and frequency of droughts decreased considerably from  
54 1998 to 2015 and wetting trends were located mainly in high-latitude areas. He concluded that at  
55 the biome level, the wetting occurred mainly in the tundra, boreal forest or taiga, and temperate  
56 coniferous forest biomes, whereas the highly drought H-vulnerable areas were mainly located in  
57 the desert and xeric shrub-land biomes. However, climate extreme events in the Arctic fluctuate  
58 and occur alternately (Przybylak 2002, 2003, Reusen et al. 2019, Overland 2020, Wash et al. 2020).

59 In recent years research indicates heterogeneity in vegetation responses to climate change  
60 in the Arctic (Myers-Smith et al. 2020). While many Arctic regions have become greener since the  
61 1980s, reflecting the positive response of tundra shrub species to warming and an increase in plant

62 growth, satellite data show a decrease in plant productivity in many areas since the early 2000s  
63 (Phoenix and Bjerke 2016; Reichle et al. 2018). The number of sites showing spectral browning  
64 in satellite studies is increasing (Berner et al. 2020), which is in line with regional field studies  
65 showing recent declines in shrub growth due to drought stress. The role of precipitation has become  
66 increasingly important in recent years, as described for Greenland (Forchhammer 2017, Gamm et  
67 al. 2018), southern Spitsbergen (Owczarek and Opała 2016), Bear Island (Owczarek et al. 2021),  
68 Iceland (Phulara et al. 2022) or Siberia (Blok et al 2011). Some regional studies show that shrubs  
69 can benefit from drier conditions, which is possibly due to a higher availability of photo-  
70 assimilates under sunny conditions (Lehejcek et al. 2006). It should be noted that severe droughts  
71 evidenced in the Arctic, have affected not only tundra browning and reduction of productivity but  
72 also resulted in the mortality of populations of species (Breshears et al. 2005, Smith 2011, Bjerke  
73 et al. 2014, Opała-Owczarek et al. 2018). On the other hand, the conditions opposite to drought  
74 (long-lasting, heavy rain events and increased summer precipitation) influence hydrologic  
75 processes, soil thermal regime and stimulates permafrost thaw (Douglas et al. 2020). The increased  
76 precipitation leads to increase solifluction rate and mass movement activity, especially debris flow  
77 events (Owczarek et al. 2013, De Hass et al. 2015; Rouyet et al. 2021). In winter the environmental  
78 impact of deficit/abundant precipitation, which can also be expressed in the form of drought  
79 indices, is different. Negative anomalies of precipitation in winter result in a reduction of snow  
80 cover depth and diminished Snow Water Equivalent (SWE) which may further lead to a negative  
81 annual mass balance of the glaciers. On the other hand, the effect of positive anomalies of winter  
82 precipitation is the opposite, i.e. increased snow accumulation, higher values of SWE and positive  
83 mass balance. Moreover, higher snow cover in the non-glaciated areas increases the avalanche risk  
84 and delays the onset of vegetation period and ground thaw (Isaksen 2007, Etzelmüller et al. 2011,  
85 Christiansen et al. 2013, Etzelmüller et al. 2011, Isaksen 2007, Kępski et al. 2017, Schuler et al.,  
86 2020).

87 Liquid precipitation in winter or winter thaws in the Arctic often described as "rain on snow  
88 events" (ROS), has negative consequences for the functioning of polar ecosystems. Rennert et al.  
89 (2009) reported that ROS events (the formation of icy layers) hamper the functioning of mammals  
90 during winter, whose populations fell as a result of restricted access to food. Bokhorst et al. (2016)  
91 and Opała-Owczarek et al. (2018) indicated the strong impact of ROS on vegetation due to the  
92 eroding effects of snow blizzards on ice-covered tundra. Łupikasza et al. (2019) found that an  
93 increase in the frequency of ROS events impacts both glacier mass balance and glacier dynamics  
94 and concluded that the total liquid precipitation during winter could be effectively stored in the  
95 glacier, contributing to 9% of the seasonal snow cover accumulation as a component of the glacier  
96 mass balance.

97 Serreze et al. (2015) stated that in Spitsbergen extreme events tend to occur when the region  
98 is influenced by a trough of low sea level pressure extending from the southwest, but some of the  
99 largest precipitation events can be associated with a 500hPa anomaly of geopotential height  
100 (positive over the Barents Sea and negative over Greenland) and positive anomalies in precipitable  
101 water with a stream extending even thousands of kilometres south into the subtropical Atlantic.  
102 This statement allows an assumption to be made that wet conditions expressed as drought indices  
103 are also related to anomalies in geopotential height and precipitable water over the North Atlantic.  
104 Thus, the hypothesis to investigate is that by contrast to conditions for extreme precipitation by  
105 Serreze et al. (2015), a deficit of atmospheric water and periods of dryness identified by negative  
106 values of the drought indices can also be explained by factors related to the distribution of baric  
107 field over the North Atlantic and regional circulation types.

108 This paper aims to recognize spatio-temporal variability of atmospheric drought impacting  
 109 ecosystems on Svalbard and identify of atmospheric circulation patterns impacting wet and dry  
 110 conditions (positive/negative values of drought indices) in the Atlantic sector of the High Arctic  
 111 as represented by Svalbard.

## 112 **2 Area, Data and Methods**

113 The deficit or excess of precipitation is described by SPEI (Standardised Precipitation  
 114 Evapotranspiration Index) by the WMO recommendations in relation to drought indices (WMO,  
 115 2016). The SPEI developed by Vicente-Serrano et al. (2010) and applied in numerous studies  
 116 (Fischer et al. 2011, Núñez et al. 2014, Stagge et al. 2015) is calculated by normalization of  
 117 climatic water balance (precipitation minus potential evapotranspiration) time series.

118 Based on the long-term climatological data from Ny Alesund (NyA), Longyearbyen - Svalbard  
 119 Airport (LYR) and Hornsund - Polish Polar Station (HOR), we undertook an analysis of drought  
 120 indices on West Spitsbergen Island, Svalbard for the period 1979-2019. The data were obtained  
 121 from the Norwegian Centre For Climate services (<https://seklima.met.no>) and from the database  
 122 published by Wawrzyniak and Osuch (2019, 2020).

123 Ny Alesund is a coastal north-westernmost station. Svalbard Airport (Longyearbyen)  
 124 represents the middle and rather continental part of the island while Hornsund Polish Polar Station  
 125 is located on the northern coast of the southernmost Hornsund fjord in Spitsbergen (Fig. 1). The  
 126 stations are operating in accordance with operative measurement regulations and standards within  
 127 the World Meteorological Organisation with the respective numbers 01007, 01008 and 01003.

128



129

130 Figure 1. Location of the study area

131 (By courtesy of the Norwegian Polar Institute, the details of the studied area are available at  
 132 <https://toposvalbard.npolar.no/?lat=78.12175&long=18.05456&zoom=1&layer=map>).

133

134 Reanalysis products provided by the NOAA / ESRL Physical Sciences Laboratory, Boulder  
 135 Colorado (<http://psl.noaa.gov>) were used to document the synoptic conditions over the North

136 Atlantic Ocean that determined the extreme pluviothermic episodes in Spitsbergen. The datasets  
137 used include composites (averages) of daily means or anomalies (deviation from long-term mean)  
138 of variables from the NCEP / NCAR Reanalysis. The plots were generated for the selected extreme  
139 values of SPEI. The following variables were used: sea level pressure, anomaly of air temperature,  
140 anomaly of 500 hPa geopotential height, omega index for 500 hPa explaining vertical motion of  
141 air mass and precipitable water anomaly between 1000-500 hPa. The influence of the regional  
142 atmospheric circulation on the SPEI values in Svalbard was assessed using the classification of  
143 atmospheric circulation types proposed by Niedźwiedź (2013, 2020).

144 Standardized Precipitation Evapotranspiration Index (SPEI) was calculated using  
145 observations of air temperature and precipitation from Ny Alesund, Longyearbyen (Svalbard  
146 Airport) and Hornsund. These meteorological variables allowed for the development of  
147 climatological water balance time series for the period 1979-2019. Potential evapotranspiration  
148 was estimated using the Hamon method based on daily air temperature and latitude of stations. A  
149 generalized Extreme Value probability distribution was fitted to the climatological water balance  
150 time series aggregated over a chosen period (annual, May-October, MAM, JJA, SON, and DJF).  
151 The same procedure was applied to all considered stations which further allowed for a comparison  
152 of the conditions between the stations. Trends in drought conditions were quantified with modified  
153 Mann-Kendall method.

154 The following SPEI classes were adopted: moderately wet  $2 < \text{SPEI} \leq 3$ ; slightly wet  $1 < \text{SPEI} \leq$   
155  $2$ ; incipient wet spell  $0.5 < \text{SPEI} \leq 1$ ; near normal  $-0.5 \leq \text{SPEI} \leq 0.5$ ; incipient dry spell  $-0.5 >$   
156  $\text{SPEI} \geq -1$ ; slightly dry  $-1 > \text{SPEI} \geq -2$ ; moderately dry  $-2 > \text{SPEI} \geq -3$ .

### 157 **3 Results and Discussion**

158 In the analyzed period 1979-2019, normal conditions ( $-0.5 \leq \text{SPEI} \leq 0.5$ ) occurred on  
159 average per year from 36.6% at Svalbard Airport to 39.0% in Ny Alesund and 41.5% in Hornsund.  
160 MAM was a season with the greatest variation in average conditions, with 53.7% at Svalbard  
161 Airport and 29.3% at Ny Alesund and Hornsund. Cases of drought ( $\text{SPEI} < -0.5$ ) most often  
162 occurred in the JJA season, i.e. 34.1% in Ny Alesund and 36.6% each in the other two stations.  
163 SON was the wettest season (with  $\text{SPEI} > 0.5$ ), with 39.0% of frequency in Hornsund, 36.6% in  
164 Ny Alesund and 26.8% of frequency in Svalbard Airport, located in the interior of the island (Table  
165 I).

166  
167 Table I. Frequency of the drought index SPEI (annual, May-October and quarter seasons MAM,  
168 JJA, SON, DJF) at Ny Alesund, Svalbard Airport and Hornsund (Spitsbergen) in the years 1979-  
169 2019.

	<b>SPEI classes</b>	<b>Annual</b>	<b>May-Oct.</b>	<b>MAM</b>	<b>JJA</b>	<b>SON</b>	<b>DJF</b>	<b>month</b>
<b>NY ALESUND</b>								
<b>No of cases</b>								
moderately wet	$2 < SPEI \leq 3$	0	1	0	1	1	2	x
slightly wet	$1 < SPEI \leq 2$	8	4	8	4	5	4	x
incipient wet spell	$0,5 < SPEI \leq 1$	5	10	7	10	9	6	x
near normal	$0,5 \geq SPEI \geq -0,5$	16	14	12	12	12	16	x
incipient dry spell	$-0,5 > SPEI \geq -1$	4	4	7	7	8	5	x
slightly dry	$-1 > SPEI \geq -2$	8	8	7	7	5	6	x
moderately dry	$-2 > SPEI \geq -3$	0	0	0	0	1	1	x
<b>% of cases</b>								
wet	$SPEI > 0,5$	31.7	36.6	36.6	36.6	36.6	30.0	x
near normal	$0,5 \geq SPEI \geq -0,5$	39.0	34.1	29.3	29.3	29.3	40.0	x
dry	$SPEI < -0,5$	29.3	29.3	34.1	34.1	34.1	30.0	x
MAX value/year		1.88/2016	2.48/2000	1.63/1990	2.15/2013	2.10/2016	2.08/2006	2.82/ V 2014
MIN value/year		-1.99/1995	-1.97/1995	-1.99/2018	-2.00/1985	-2.29/1995	-2.20/2000	-3.00/ IV 2006
<b>SVALBARD AIRPORT</b>								
<b>No of cases</b>								
moderately wet	$2 < SPEI \leq 3$	1	1	2	1	1	1	x
slightly wet	$1 < SPEI \leq 2$	6	6	3	5	4	5	x
incipient wet spell	$0,5 < SPEI \leq 1$	5	7	6	10	6	8	x
near normal	$0,5 \geq SPEI \geq -0,5$	15	17	22	10	19	13	x
incipient dry spell	$-0,5 > SPEI \geq -1$	7	3	4	10	7	4	x
slightly dry	$-1 > SPEI \geq -2$	7	7	2	4	3	9	x
moderately dry	$-2 > SPEI \geq -3$	0	0	2	1	1	0	x
<b>% of cases</b>								
wet	$SPEI > 0,5$	29.3	34.1	26.8	39.0	26.8	35.0	x
near normal	$0,5 \geq SPEI \geq -0,5$	36.6	41.5	53.7	24.4	46.3	32.5	x
dry	$SPEI < -0,5$	34.1	24.4	19.5	36.6	26.8	32.5	x
MAX value/year		2.33/1981	2.18/1981	2.49/1993	2.39/1981	2.76/2016	2.07/1996	2.84/ IV 1990
MIN value/year		-1.96/1998	-1.69/2009	-2.92/2006	-2.10/2007	-2.60/1995	-1.78/1987	-3.77/ IV 2006
<b>HORNSUND</b>								
<b>No of cases</b>								
moderately wet	$2 < SPEI \leq 3$	2	1	1	0	1	1	x
slightly wet	$1 < SPEI \leq 2$	3	5	6	6	5	5	x
incipient wet spell	$0,5 < SPEI \leq 1$	6	7	8	5	10	5	x
near normal	$0,5 \geq SPEI \geq -0,5$	17	13	12	15	12	17	x
incipient dry spell	$-0,5 > SPEI \geq -1$	8	7	6	6	4	9	x
slightly dry	$-1 > SPEI \geq -2$	3	7	6	9	8	3	x
moderately dry	$-2 > SPEI \geq -3$	2	1	2	0	1	1	x
<b>% of cases</b>								
wet	$SPEI > 0,5$	26.8	31.7	36.6	26.8	39.0	26.8	x
near normal	$0,5 \geq SPEI \geq -0,5$	41.5	31.7	29.3	36.6	29.3	41.5	x
dry	$SPEI < -0,5$	31.7	36.6	34.1	36.6	31.7	31.7	x
MAX value/year		2.29/2016	2.00/1994	2.31/1982	1.92/1994	2.16/2016	2.46/1996	2.81/ IV 1992
MIN value/year		-2.35/2019	-2.13/1987	-2.15/2019	-1.77/2017	-2.07/1983	-2.64/1988	-2.96/ IV 2006

170

171

172

173

174

175

176

177

178

Trends in drought conditions were quantified with modified Mann-Kendall method and are presented in Table II. Statistically significant changes were estimated for various periods depending on stations. An agreement in trend directions between Ny Alesund and Hornsund even in the case of insignificant trends. At these two stations (NyA, HOR) positive trends indicating wetter conditions dominated while in Longyearbyen (LYR) negative trends were significant indicating progressive dryness. Significant trends in the same direction at least at two stations were found in MAM, SON and DJF. The largest changes were estimated for autumn where negative

179 values of SPEI occur more often in the first part of the period and positive values dominate in the  
 180 last 20 years.

181

182 Table II. The results of trend analysis with modified Mann-Kendall method for SPEI.

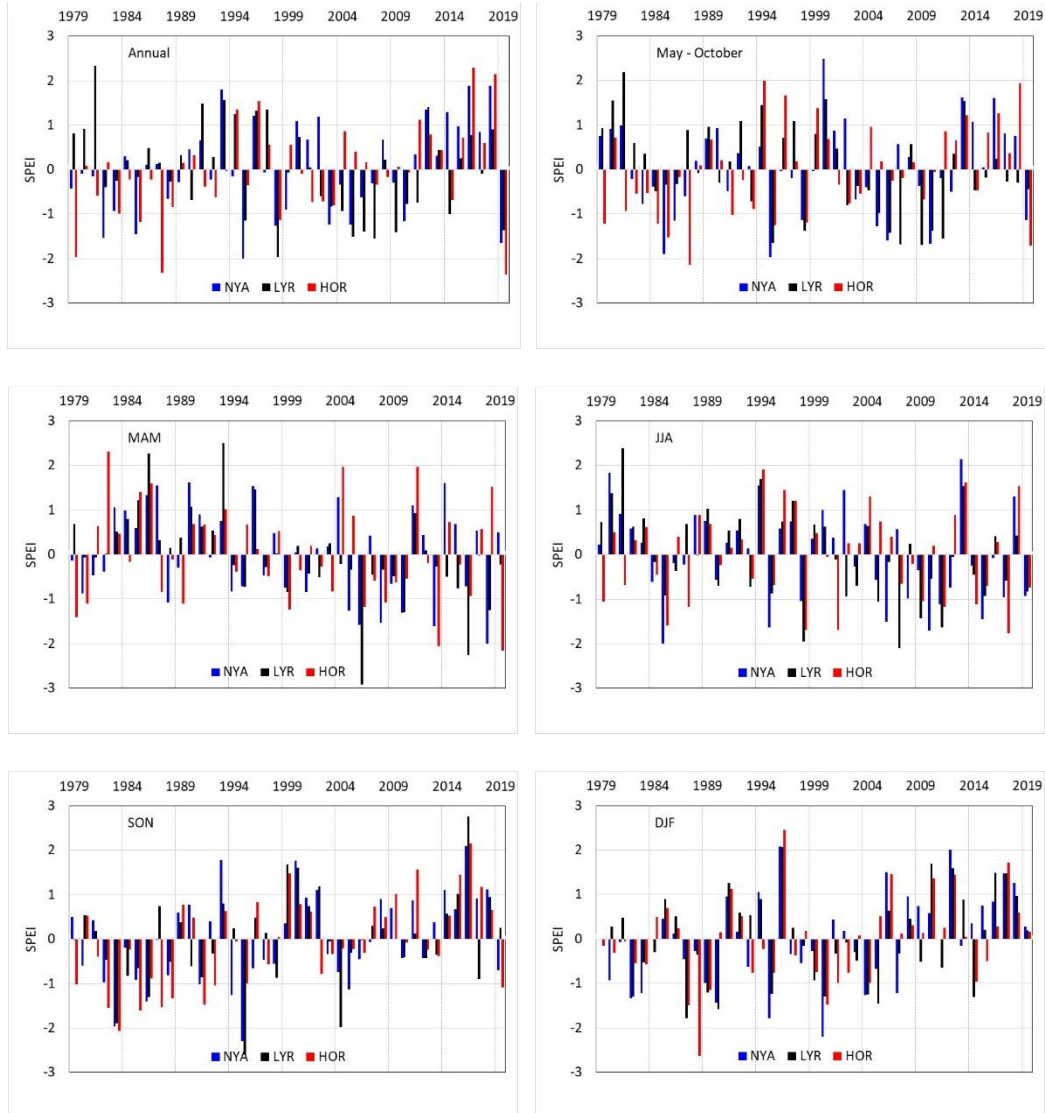
	SPEI (change per decade)					
	Ny Alesund (NYA)		Svalbard Airport (LYR)		Hornsund (HOR)	
	Slope of trend	p-value	Slope of trend	p-value	Slope of trend	p-value
annually	0.3032	0.0817	-0.2724	0.0817	<b>0.3326</b>	0.0376
May-Oct	0.0566	0.6855	<b>-0.3650</b>	0.0147	<b>0.3033</b>	0.0398
MAM	-0.1637	0.2860	<b>-0.3601</b>	2.1962e-04	<b>-0.2285</b>	1.3323e-15
JJA	-0.2578	0.1082	<b>-0.3494</b>	0.0095	-0.0858	0.3399
SON	<b>0.3148</b>	0.0101	0.2005	0.1133	<b>0.4821</b>	8.5028e-04
DJF	<b>0.3801</b>	0.0066	0.1829	0.2487	<b>0.1820</b>	0.0065

183

184 The SPEI values were characteristic of big inter-seasonal variability (Fig. 2). In a particular season  
 185 , all stations usually experienced the same conditions (dry or wet) but of various intensities. The  
 186 seasons with extremely different conditions at the stations were rare.

187 In the studied period, it was possible to indicate several-year long periods with the SPEI of the  
 188 same sign (plus or minus) indicating a domination of drought or wet conditions. Long-term  
 189 variability of annual and half-year (May-October) values of SPEI showed a prevalence of droughts  
 190 in 80-ties and the first decade of the 21<sup>st</sup> century while wet seasons were frequent in 90-ties and  
 191 the second decade of the 21<sup>st</sup> century. Seasonal SPEIs were characteristic of great inter-annual  
 192 variability. In MAM and JJA droughts were more frequent after 2000, in the same period in SON  
 193 and DJF the frequency of wet seasons increased. The most remarkable changes in the scale of the  
 194 entire research period were estimated for autumn where negative values of SPEI occur more often  
 195 in the first part of the period and positive values dominate in the last 20 years.

196

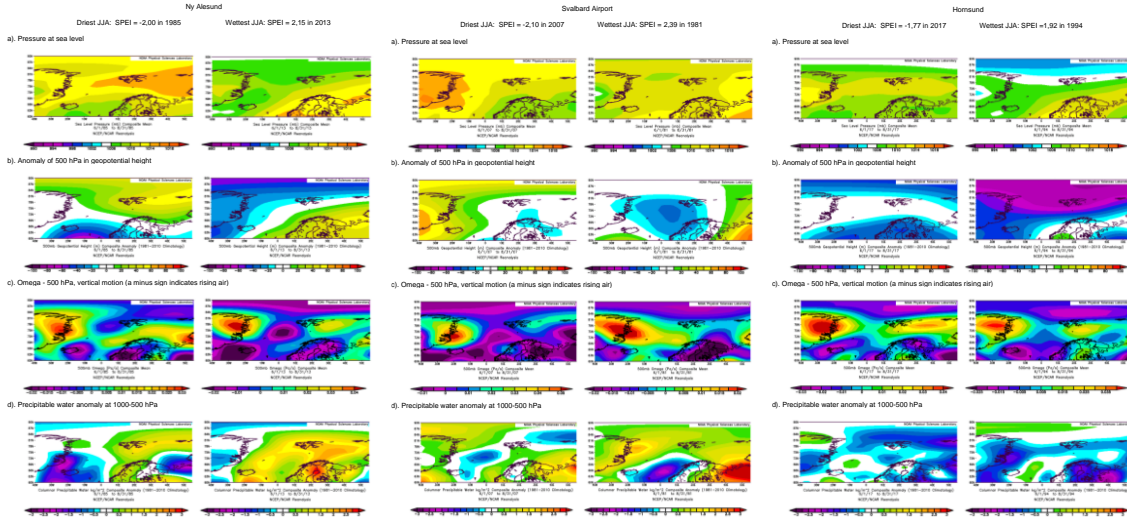


197  
 198 Figure 2. The Standardised Precipitation Evapotranspiration Index SPEI (annual, May-October  
 199 and quarter seasons MAM, JJA, SON, DJF) at Ny Alesund, Longyearbyen and Hornsund, W  
 200 Spitsbergen in the years 1979-2019.

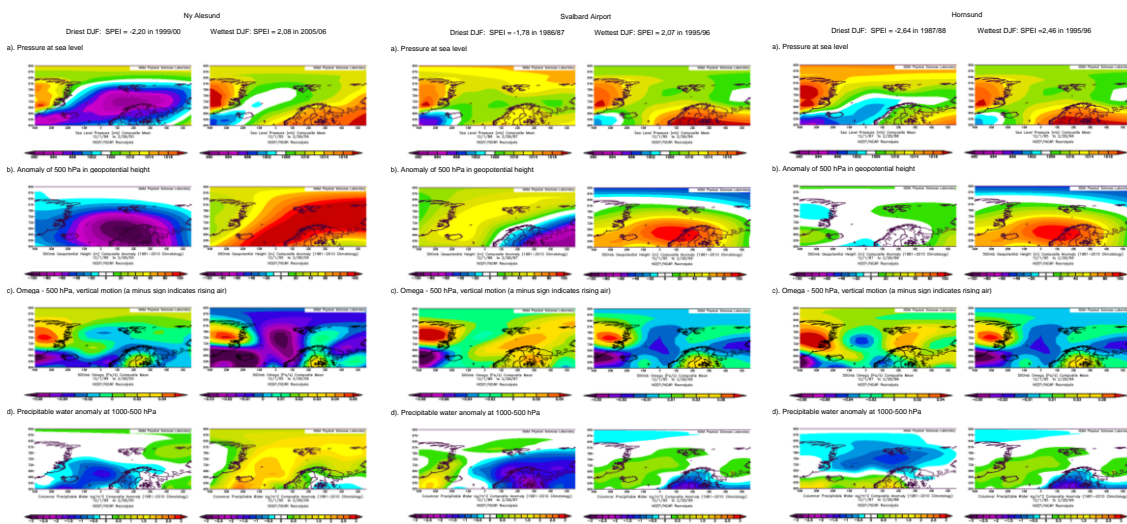
201 *Drought classes (DC): moderately wet  $2 < DC \leq 3$ ; slightly wet  $1 < DC \leq 2$ ; incipient wet*  
 202 *spell  $0,5 < DC \leq 1$ ; near normal  $-0,5 \leq DC \leq 0,5$ ; incipient dry spell  $-0,5 > DC \geq -1$ ; slightly*  
 203 *dry  $-1 > DC \geq -2$ ; moderately dry  $-2 > DC \geq -3$ .*

204

205 Extending the findings by Serreze et al. (2015) on conditions favouring the extreme  
 206 precipitation occurrence in the Arctic, we assume that dry conditions identified with SPEI also  
 207 depend on of the patterns of geopotential height and precipitable water over the Atlantic sector of  
 208 the Arctic. The atmospheric conditions over the N Atlantic which occurred during months with  
 209 the most extreme SPEI values in summer and winter in Ny Alesund, in Svalbard  
 210 Airport/Longyearbyen and Hornsund are presented in Figures 3 and 4.



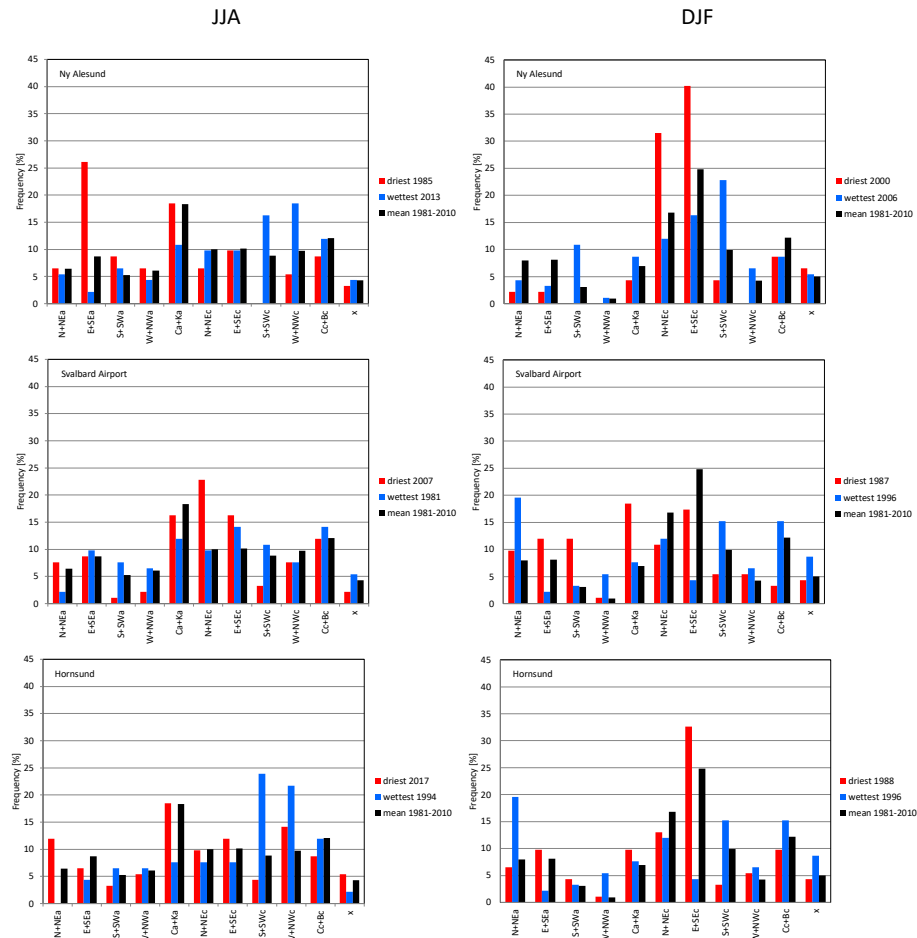
211  
 212 Figure 3. The atmospheric conditions over the N Atlantic formed in summer (JJA) the most  
 213 extreme values of drought conditions in Ny Alesund, Svalbard Airport and Hornsund, W  
 214 Spitsbergen. Image provided by the NOAA/ESRL Physical Sciences Laboratory, Boulder  
 215 Colorado from their Web site at <http://psl.noaa.gov> and submitted 10 December 2021.



216  
 217 Figure 4. The atmospheric conditions over the N Atlantic formed in winter (DJF) the most  
 218 extreme values of drought conditions in Ny Alesund, Svalbard Airport and Hornsund, W  
 219 Spitsbergen. Image provided by the NOAA/ESRL Physical Sciences Laboratory, Boulder  
 220 Colorado from their Web site at <http://psl.noaa.gov> and submitted 22 January 2022.

221  
 222 Both extreme precipitation events and wet conditions expressed by high positive values of  
 223 SPEI drought index depend on anomalies of 500 hPa geopotential height and precipitable water  
 224 determined by the baric field over the North Atlantic. By contrast, a deficit of atmospheric water  
 225 and periods of dryness are expressed by negative values of the drought indices. In DJF situations  
 226 like these are formed over Svalbard when an area of high pressure develops with centres located  
 227 over the Greenland and central Arctic reaching the Barents Sea (advection from the eastern sector)

228 and blocking the transport of moisture usually associated with cyclonic advection of air masses  
 229 from the S+SW sector (Fig. 4). In summer dry conditions are associated with the ridge of high  
 230 pressure or extended area of increased pressure between the Greenland Sea and the Barents Sea.  
 231 The dominating anticyclonic conditions block the intrusion of mid-latitude lows and related  
 232 transport of wet air masses. Convection that favours extreme rainfall weakens under high-pressure  
 233 conditions (close to 0 anomalies of Omega-500hPa) and the development of the anticyclonic  
 234 conditions blocks the increase in precipitable water in the atmosphere and consequently inhibits  
 235 the precipitation process and reduces the amount of rain. The low-pressure zone is then shifted to  
 236 the south and stretches along the trajectories of the atmospheric fronts moving latitudinally from  
 237 Iceland towards Scandinavia. The position of the lows is marked by a 500 hPa anomaly of  
 238 geopotential height. The conditions favouring the occurrence of extreme precipitation which  
 239 determine high SPEI values have been recognized by Serreze et al. (2015) for short-term states of  
 240 the atmosphere. Such criteria averaged over relatively long JJA and DJF seasons, on the one hand,  
 241 show a large spatial diversity, but on the other hand, the features proving their driving role become  
 242 less clear. Therefore, in the next step, the circulation types are analysed as decisive for the  
 243 occurrence of extremely dry and wet conditions in JJA and DJF, when the drought or water  
 244 abundance is crucial for vegetation, ablation and melting of the active layer of permafrost (in JJA)  
 245 or snowfall resources (in DJF) (Figure 5).  
 246



249

250 Figure 5. The frequency of atmospheric circulation types in the JJA and DJF seasons with the  
251 lowest and the highest values of SPEI vs climatic normal 1981-2010.

252

253 At analysed stations located in the distance of more than 200 km from each other, representing the  
254 northern, middle and southern parts of western Spitsbergen the most extreme values of drought  
255 conditions developed under the influence of various circulation types. However, it was possible to  
256 find some similarities in the patterns of circulation types frequency favouring extremely wet and  
257 dry conditions between Ny Alesund and Hornsund, both having more maritime climate than  
258 Longyearbyen. In summer (JJA) the driest episode in Ny Alesund occurred during anticyclonic  
259 circulation (a) with air advection from E+SE sector (type E+SEa) followed by the centre of high  
260 or high-pressure ridge over Svalbard (type Ca+Ka) that also favoured the occurrence of dry  
261 episodes in the south at Hornsund station due to more stable anticyclonic conditions or descending  
262 air in the Ca centre. Moreover, in Hornsund, dry episodes were related to advection of cold and  
263 dry air from N+NE (type N+NEa) under an influence of anticyclone which prevents convection,  
264 and to cyclonic types W+NW. According to previous studies type NWc insignificantly correlated  
265 with air temperature (Łupikasza and Niedźwiedź 2020) and is characteristic of low precipitation  
266 totals (Łupikasza 2013). In Longyearbyen dry conditions were primarily related to cyclonic  
267 circulation (c) from N+NE (type N+NEc) sector, followed by E+SEc and Ca+Ka types.

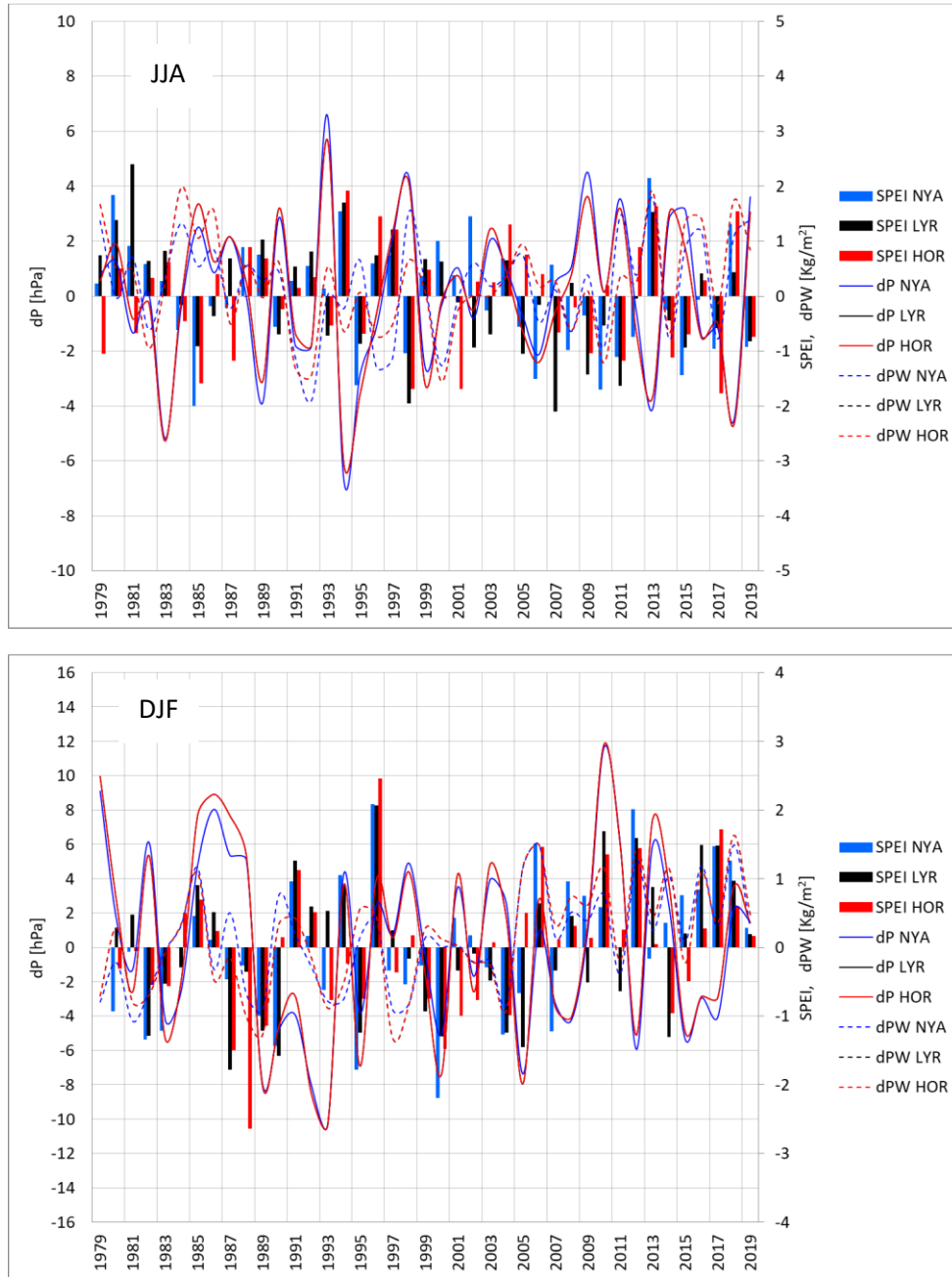
268 In Ny Alesund during extremely wet seasons cyclonic situation (c) with W+NW and S+SW  
269 advection dominated. The same types prevailed during drought in Hornsund; however, during the  
270 wettest episode in JJA 1994 the frequency of S+SWc type was higher than W+NWc. It is  
271 reasonable to state that it was S+SWc that generated extremely wet conditions at these stations.  
272 Many papers prove the increased precipitation over Svalbard during air advection from the  
273 southern sector (Łupikasza 2008, Łupikasza 2013, Dobler et al 2021).

274 In central Spitsbergen (Longyearbyen) JJA extremely wet conditions resulting from high  
275 frequency of cyclone centre or trough of low pressure (type Cc+Bc) which are both conducive to  
276 convection and an advection of warm and wet air masses from the E+SE sector.

277 In Ny Alesund, most dry winter (DJF) was due to cyclonic advection of cold and dry air from  
278 N+NE and warmer but also dry air from E+SE which intensified evaporation. The wettest DJF  
279 developed under cyclonic circulation (c) and increased compared to average, frequency of air  
280 advection from S+SW sector. Regardless of baric type, the air masses from S sector, particularly  
281 from SW are warmer and wetter than the arctic air. The driest conditions in the central part of  
282 Svalbard appeared during the existence of the ridge of high pressure or high with its centre located  
283 over Svalbard. (type Ca+Ka) and, like in the north, during cyclonic circulation (c) from E+SE  
284 sector. In that part of Svalbard, and in the south (Hornsund), high values of SPEI were favoured  
285 by S+SWc type (the occurrence of precipitation) and the anticyclonic N+NEa type (low  
286 evaporation due to low temperatures). Interestingly, in both locations, the frequency of N+NEa  
287 type was high during the extremely wet episode in 1996.

288 Concluding, averaged over the JJA and DJF seasons the mean state of the atmosphere during  
289 extremely dry conditions indicates that only the anticyclonic conditions, particularly the K+Ca  
290 type and air advection from the N sector and negative anomalies of precipitable water are decisive  
291 for dry conditions in contrast to wet conditions which are driven by positive anomalies of  
292 precipitable water and cyclonic conditions. These results were proved by the frequency of regional  
293 circulation types during the JJA and DJF seasons with the lowest and the highest values of SPEI.  
294 Figure 6 shows long-term variability in the anomalies of sea level pressure and precipitable water

295 for summer (JJA) and winter (DJF) seasons in the northern part of the research area (Ny Alesund),  
 296 central (Longyearbyen) and southern part of Svalbard (Hornsund).  
 297



298  
 299 Figure 6. SPEI in summer (JJA) and winter (DJF) and anomalies of mean atmospheric pressure  
 300 and precipitable water (vs climatic normal 1981-2010) in Ny Alesund (NYA), Longyearbyen  
 301 (LYR) and Hornsund (HOR). Image provided by the NOAA/ESRL Physical Sciences Laboratory,  
 302 Boulder Colorado from their Web site at <http://psl.noaa.gov> and submitted 28 January 2022.

303  
 304

305 The long-term course of the variables in subsequent seasons between 1979-2019 indicates strong  
 306 relationships between the SPEI drought index and anomalies of precipitable water (PW) and  
 307 somewhat weaker relationships with anomalies of sea level pressure. As long as the differences in  
 308 the anomalies of atmospheric pressure between the stations can be considered as insignificant, the  
 309 anomalies of precipitable water during dry conditions in Ny Alesund differed from those in  
 310 Longyearbyen and Hornsund both having similar patterns of atmospheric conditions favouring  
 311 droughts occurrence.

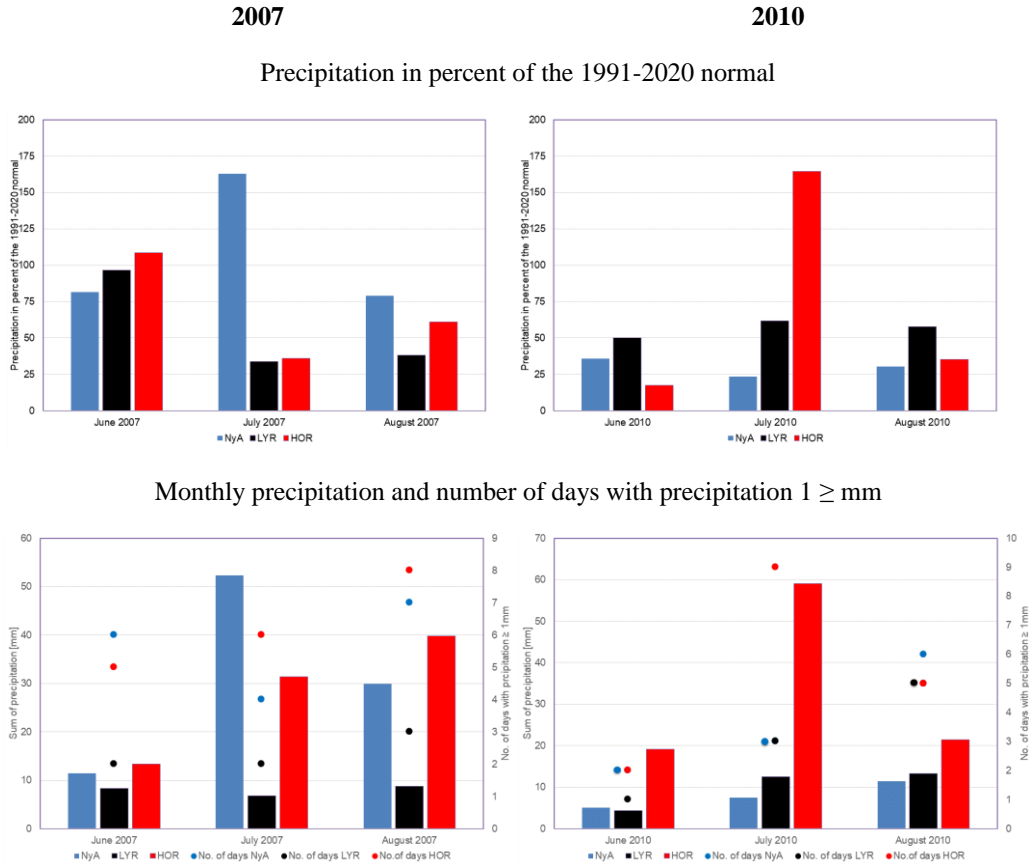
312 During most of the analysed period the dry and wet situations occurred alternatively as mesoscale  
 313 phenomena appearing simultaneously over the entire Spitsbergen in particular years (Figure 2 and  
 314 Figure 6). However, in the case of several years the extreme conditions were found in the same  
 315 year, e.g. drought in the north wet conditions in the south or opposite. In the period 1979-2019 the  
 316 months with uniform wet-dry conditions constituted from 39% to 41.5% cases for both seasons,  
 317 while the contrast conditions were represented by one-third cases (24.4%-26.8%) (Table III).  
 318

319 Table. III. Years with extreme SPEI values in July, summer and winter in Ny Alesund,  
 320 Longyearbyen and Hornsund.

SPEI JULY				SPEI JJA				SPEI DJF			
Year	NyA	LYR	HOR	Year	NyA	LYR	HOR	Year	NyA	LYR	HOR
1986	-0.54	-0.28	1.07	1979	0.23	0.74	-1.05	1980	-0.93	0.28	-0.31
1991	0.94	-0.03	-0.66	1987	-0.22	0.68	-1.17	1993	-0.62	0.53	-0.77
1992	0.34	-0.10	-0.99	2000	1.00	0.63	-0.05	1994	1.05	0.89	-0.23
2001	-0.65	0.24	-0.86	2001	0.38	-0.11	-1.69	2001	0.43	-0.33	-0.99
2002	1.27	-0.78	-0.42	2002	1.45	-0.94	0.26	2005	-0.67	-1.45	0.51
2007	1.03	-1.34	-0.75	2005	-0.56	-1.05	0.75	2007	-1.22	-0.33	0.12
2008	-0.59	0.72	-0.35	2006	-1.51	-0.16	0.4	2009	0.75	-0.51	0.13
2010	-1.24	-0.26	0.77	2007	0.57	-2.1	-0.66	2013	-0.16	0.88	0.04
2012	-0.74	0.23	0.32	2008	-0.99	0.24	-0.21	2014	0.35	-1.3	-0.96
2017	0.38	0.16	-0.85	2010	-1.7	-0.54	0.2	2015	0.76	0.2	-0.5
				2012	-0.74	-0.04	0.89				

321  
 322 For two reasons special attention has been focused on SPEI values for the summer season (JJA)  
 323 and its individual summer months. It was assumed that the analysis of atmospheric conditions on  
 324 a monthly scale help to explain spatial variations in wet/dry conditions. Moreover, the analysis on  
 325 a monthly scale enables description of the relationships between SPEI and tundra vegetation. To  
 326 do so, July was selected when the intense development of vegetation is not limited by snow cover  
 327 like in June.

328 The contrasts in wet/dry conditions over Svalbard are well represented by the summers of 2007  
 329 and 2010. In the summer 2007, particularly in July the northern part of Svalbard (Ny Alesund)  
 330 with slightly wet conditions (SPEI = 1.03) strongly contrasted with the drought that appeared in  
 331 the central (Longyearbyen, SPEI: -1.34, slightly dry) and south-western Svalbard (Hornsund, SPEI  
 332 = -0.75). In July 2010 the situation was opposite i.e. drought in the north (Ny Alesund, SPEI = -  
 333 1.24) and incipient wet spell in the vicinity of Hornsund (SPEI = 0.77), and near normal conditions  
 334 in Longyearbyen (SPEI = -0.26). Figure 7 illustrates the precipitation differences between analysed  
 335 stations in the summer seasons 2007 and 2010. The atmospheric conditions over Svalbard during  
 336 contrasting conditions in the summer July 2007 and 2010 are presented in Figure 8.  
 337



338  
339  
340  
341  
342

Figure 7. Monthly precipitation in summer seasons 2007 and 2010 in Ny Alesund, Longyearbyen and Hornsund (Figure based on the data from the Norwegian Centre For Climate services (<https://seklima.met.no>) submitted 24 of February 2022).

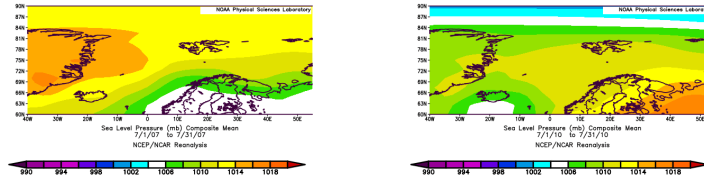
July 2007

SPEI: NYA 1,03; LYR -1,34; HOR -0,75

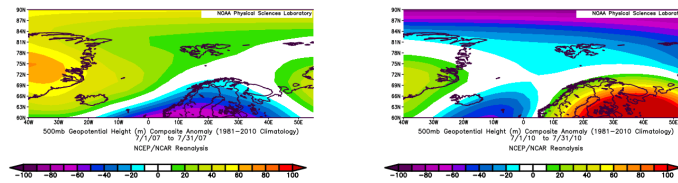
July 2010

SPEI: NYA -1,24; LYR -0,26; HOR 0,77

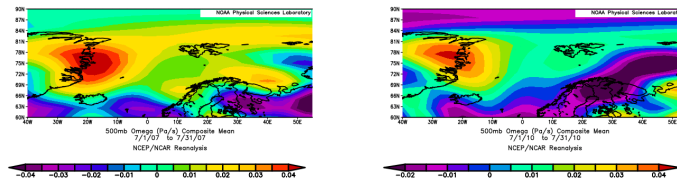
a). Pressure at sea level



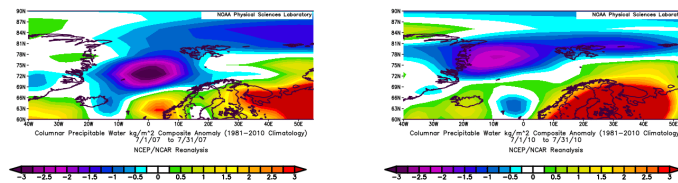
b). Anomaly of 500 hPa in geopotential height



c). Omega - 500 hPa, vertical motion (a minus sign indicates rising air)



d). Precipitable water anomaly at 1000-500 hPa



343

344 Figure 8. The atmospheric conditions over the N Atlantic formed in July 2007 and 2010 the most  
 345 extreme contrasts of drought conditions between Ny Alesund, Svalbard Airport and Hornsund, W  
 346 Spitsbergen. Image provided by the NOAA/ESRL Physical Sciences Laboratory, Boulder  
 347 Colorado from their Web site at <http://psl.noaa.gov> and submitted 11 of February 2022.

348

349 Contrasts of SPEI in July 2007 and 2010 were due to diverse precipitation in the north compared  
 350 to the south part of Svalbard. The total July precipitation in Ny Alesund in 2007 exceeded 160%  
 351 of 1991-2020 average, while in Longyearbyen and Hornsund the precipitation totals reached 33-  
 352 35% of the average. In 2010 situation was opposite i.e. in Hornsund the total precipitation in July  
 353 reached 164% of the climatic norm, in Longyearbyen - 62%, and in Ny Alesund the total reached  
 354 only one fourth of the norm (23.4%) calculated as average from the period 1991-2020.

355 Slightly wet conditions in northern Svalbard (Ny Alesund) and simultaneously slightly dry  
356 conditions in the central part and incipient dry spell in the south developed under an influence of  
357 the ridge of high pressure related to the well-expanded high with its centre over the southern part  
358 of Scandinavian Peninsula. Such a distribution of air pressure forced the air masses to inflow over  
359 central and southern Svalbard from over the Barents Sea causing negative anomalies of perceptible  
360 water over the Greenland Sea. At the same time, in the northern part of Svalbard is under an  
361 influence of anticyclone circulation prevailed the conditions that favoured the development of air  
362 temperature inversions and low stratiformis cloudiness and drizzle.

363

#### 364 **4 Conclusions**

365 In the analyzed period 1979-2019, normal conditions ( $-0.5 \leq \text{SPEI} \leq 0.5$ ) occurred on  
366 average per year from 36.6% at Svalbard Airport to 39.0% in Ny Alesund and 41.5% in Hornsund.  
367 MAM was a season with the greatest variation in average conditions, as 53.7% at Svalbard Airport  
368 and 29.3% at Ny Alesund and Hornsund. Cases of drought ( $\text{SPEI} < -0.5$ ) most often occurred in  
369 the JJA season, i.e. 34.1% in Ny Alesund and 36.6% each in the other two stations. SON was the  
370 wettest season (with  $\text{SPEI} > 0.5$ ), with 39.0% of frequency in Hornsund, 36.6% in Ny Alesund and  
371 26.8% of frequency in Svalbard Airport, located in the interior of the island.

372 In the studied period, it was possible to indicate several-year long periods with the SPEI of  
373 the same sign (plus or minus) indicating a domination of drought or wet conditions. Long-term  
374 variability of annual and half-year (May-October) values of SPEI showed a prevalence of droughts  
375 in 80-ties and in the first decade of the 21<sup>st</sup> century while wet seasons were frequent in 90-ties and  
376 in second decade of the 21<sup>st</sup> century. Seasonal SPEIs were characteristic of great inter-annual  
377 variability. In MAM and JJA droughts were more frequent after 2000; in the same period in SON  
378 and DJF the frequency of wet seasons increased. The most remarkable changes in the scale of the  
379 entire research period were estimated for autumn where negative values of SPEI occur more often  
380 in the first part of the period and positive values dominate in the last 20 years.

381 During most of the analysed periods the dry and wet situations occurred alternatively as  
382 mesoscale phenomena appearing simultaneously over the entire Spitsbergen in particular years.  
383 The extreme conditions occurred for various years at each station. In the NW part of Spitsbergen  
384 (Ny Alesund) the driest summer appeared in 1998 ( $\text{SPEI} -2.00$ ), while an extremely wet summer  
385 was that in 2013 with SPEI value of  $-2.15$ . In the central part of Spitsbergen (Svalbard  
386 Airport/Longyearbyen) the extreme summers occurred in 2007 with drought index equal to  $-2.10$   
387 and in 1981 with the highest ESPI value of  $2.39$ . In Hornsund representing the South of  
388 Spitsbergen, the driest summer season (JJA) was that in 2017 with SPEI value of  $-1.77$  and the  
389 wettest JJA occurred in 1994 with SPEI equal to  $1.92$ . In Ny Aalesund the driest winter (DJF)  
390 occurred in 1999/00 with SPEI  $-2.20$ . The winter season 005/06 was extremely wet. In  
391 Longyearbyen the extreme seasons were in 1986/87 ( $\text{SPEI} -1.78$ ) and 1995/96 ( $\text{SPEI} 2.07$ ). In the  
392 south of Spitsbergen, in Hornsund extremely wet winter overlapped with that in Longyearbyen  
393 (1995/96 with  $\text{SPEI} 2.07$ ). During the driest winter of 1987/88 SPEI reached  $-2.64$ .

394 Both extreme precipitation events and wet conditions expressed by high positive values of  
395 SPEI drought index depend on anomalies of 500 hPa geopotential height and precipitable water  
396 determined by the baric field over the North Atlantic. By contrast, a deficit of atmospheric water  
397 and periods of dryness are expressed by negative values of the drought indices. In DJF situations  
398 like these are formed over Svalbard when an area of high pressure develops with centres located

399 over the Greenland and central Arctic reaching the Barents Sea (advection from the eastern sector)  
 400 and blocking the transport of moisture usually associated with cyclonic advection of air masses  
 401 from the S+SW sector. In summer dry conditions are associated with ridge of high pressure or an  
 402 extended area of increased pressure between the Greenland Sea and the Barents Sea.

403 Averaged over the JJA and DJF seasons the mean state of the atmosphere during extremely  
 404 dry conditions indicates that only the anticyclonic conditions, particularly the K+Ca type and air  
 405 advection from the N sector and negative anomalies of precipitable water are decisive for dry  
 406 conditions in contrast to wet conditions which are driven by positive anomalies of precipitable  
 407 water and cyclonic conditions. These results were proved by the frequency of regional circulation  
 408 types during the JJA and DJF seasons with the lowest and the highest values of SPEI.

409 At analysed stations located in a distance of more than 200 km from each other,  
 410 representing the northern, middle and southern part of western Spitsbergen the most extreme  
 411 values of drought conditions developed under the influence of various circulation types. However,  
 412 it was possible to find some similarities in the patterns of circulation types frequency favouring  
 413 extremely wet and dry conditions between Ny Alesund and Hornsund, both having more maritime  
 414 climate than Longyearbyen.

## 415 **Acknowledgments**

416 The results presented in this paper were obtained within the project No. 2021/41/B/ST10/03381  
 417 “Spatio-temporal patterns in Arctic tundra greening and browning – identification of key  
 418 environmental factors (TURNING)” and the project No. 2017/27/B/ST10/01269,  
 419 “Reconstructions and projections of the hydro-climatic conditions of southern Spitsbergen”, both  
 420 financed by the Polish National Science Centre.  
 421

## 422 **References**

- 423 Anderson, J.N., Saros, J.E., Bullard, J.E., Cahoon, S.M.P., McGowan, S., Bagshaw, E.A. et al.  
 424 (2017), The Arctic in the Twenty-First Century: Changing Biogeochemical Linkages  
 425 across a Paraglacial Landscape of Greenland. *BioScience*, 67(2), 118-133. doi:  
 426 10.1093/biosci/biw158.
- 427 Berner L.T., Massey R., Jantz P., Forbes B.C., Macias-Fauria M., Myers-Smith I. et al. (2020),  
 428 Summer warming explains widespread but not uniform greening in the Arctic tundra  
 429 biome. *Nat. Commun.*, 11,1-12. doi:10.1038/s41467-020-18479-5.
- 430 Biskaborn, B.K., Smith, S.L., Noetzli, J., Matthes, H., Vieira G., Streletskiy, D.A. et al. (2019),  
 431 Permafrost is warming at a global scale. *Nature Communications*, 10, 264. doi:  
 432 10.1038/s41467-018-08240-4.
- 433 Bjerke, J.W., Karlsen, S.R., Tommervik, H. (2014), Record-low primary productivity and high  
 434 plant damage in the Nordic Arctic Region in 2012 caused by multiple weather events and  
 435 pest outbreaks. *Environmental Research Letters*, 9(8). doi: 10.1088/1748-  
 436 9326/9/8/084006.
- 437 Blok, D., Sass-Klaassen, U., Schaepman-Strub, G., Heijmans, M.M.P.D., Sauren, P., Berendse,  
 438 F. (2011), What are the main climate drivers for shrub growth in Northeastern Siberian  
 439 tundra? *Biogeosciences*, 8(5) 1169–1179. doi:10.5194/bg-8-1169-2011.

- 440 Bokhorst, S., Pedersen, S.H., Brucker, L., et al. (2016), Changing Arctic snow cover: a review of  
 441 recent developments and assessment of future needs for observations, modelling, and  
 442 impacts. *Ambio*, 45,516–537. doi: 10.1007/s13280-016-0770-0.
- 443 Breshears, D.D., Cobb, N.S., Rich, P.M., Price, K.P., Allen, C.D., Balice, R.G. et al. (2005),  
 444 Regional vegetation die-off in response to global-change type drought. *Proceedings of the*  
 445 *National Academy of Science USA*, 102(42),15144–15148. doi: 10.1073/pnas.0505734102.
- 446 Christiansen, H.H., Humlum, O., Eckerstorfer, M. (2013), Central Svalbard 2000–2011  
 447 Meteorological Dynamics and Periglacial Landscape Response. *Arctic, Antarctic, and*  
 448 *Alpine Research*, 45(1), 6–18. doi: 10.1657/1938-4246-45.1.6.
- 449 De Haas, T., Kleinhans, M. G., Carbonneau, P. E., Rubensdotter, L., Hauber, E. (2015), Surface  
 450 morphology of fans in the high-Arctic periglacial environment of Svalbard: Controls and  
 451 processes, *Earth Sci. Rev.*, 146, 163– 182. doi:10.1016/j.earscirev.2015.04.004.
- 452 Dobler, A., Lutz J., Landgren, O., Haugen, J.E. (2021), Circulation Specific Precipitation Patterns  
 453 over Svalbard and Projected Future Changes. *Atmosphere*, 11(12), 1378. doi:  
 454 10.3390/atmos11121378.
- 455 Douglas, T.A., Turetsky, M.R., Koven, C.D. (2020), Increased rainfall stimulates permafrost  
 456 thaw across a variety of Interior Alaskan boreal ecosystems. *npj Clim Atmos Sci.*, 3 (28).  
 457 doi: 10.1038/s41612-020-0130-4.
- 458 Etzelmüller, B., Schuler, T. V., Isaksen, K., Christiansen, H. H., Farbrøt, H., Benestad, R.E.  
 459 (2011), Modelling the temperature evolution of Svalbard permafrost during the 20th and  
 460 21st century. *The Cryosphere*, 5, 67-79. doi: 10.5194/tc-5-67-2011.
- 461 Fisher, J.B., Whittaker, R.J., Malhi, Y. (2011), ET come home: potential evapotranspiration in  
 462 geographical ecology. *Global Ecol. Biogeogr.*, 20, 1–18. doi: 10.1111/j.1466-  
 463 8238.2010.00578.x.
- 464 Forchhammer, M. (2017), Sea-ice induced growth decline in Arctic shrubs. *Biol. Lett.* 13(8),  
 465 20170122. doi: 10.1098/rsbl.2017.0122.
- 466 Gamm, C.M., Sullivan, P.F., Buchwal, A., Dial, R.J., Young, A.B., Watts, D.A. et al. (2018),  
 467 Declining growth of deciduous shrubs in the warming climate of continental western  
 468 Greenland. *J. Ecol.*, 106, 640–654. doi:10.1111/1365-2745.12882.
- 469 Hinzman, L.D., Deal, C.J., McGuire, A.D., Mernild, S.H., Polyakov, I.V., Walsh, J.E. (2013),  
 470 Trajectory of the Arctic as an integrated system. *Ecological Applications*, 23(8): 1837-  
 471 1868. doi: 10.1890/11-1498.1.
- 472 IPCC. (2019), Summary for Policymakers. In: *IPCC Special Report on the Ocean and Cryosphere*  
 473 *in a Changing Climate* [H.O. Pörtner, D.C. Roberts, V. Masson-Delmotte, P. Zhai, M.  
 474 Tignor, E. Poloczanska, K. Mintenbeck, A. Alegría, M. Nicolai, A. Okem, J. Petzold, B.  
 475 Rama, N.M. Weyer (eds.)]. Cambridge University Press, Cambridge, UK and New York,  
 476 NY, USA, pp. 3–35. doi:10.1017/9781009157964.001.
- 477 IPCC. (2021), Summary for Policymakers. In: *Climate Change 2021: The Physical Science*  
 478 *Basis. Contribution of Working Group I to the Sixth Assessment Report of the*  
 479 *Intergovernmental Panel on Climate Change* [Masson-Delmotte, V., P. Zhai, A. Pirani,  
 480 S.L. Connors, C. Péan, S. Berger, N. Caud, Y. Chen, L. Goldfarb, M.I. Gomis, M. Huang,  
 481 K. Leitzell, E. Lonnoy, J.B.R. Matthews, T.K. Maycock, T. Waterfield, O. Yelekçi, R.  
 482 Yu, and B. Zhou (eds.)]. Cambridge University Press, Cambridge, United Kingdom and  
 483 New York, NY, USA, pp. 3–32. doi:10.1017/9781009157896.001.

- 484 Isaksen, K., Sollid, J. L., Holmlund, P., and Harris, C. (2007), Recent warming of mountain  
485 permafrost in Svalbard and Scandinavia, *Journal of Geophysical Research–Earth*, 112  
486 (F2), F02S04. doi:10.1029/2006JF000522.
- 487 Kępski, D., Luks, B., Migała, K., Wawrzyniak, T., Westermann, S., Wojtuń, B., 2017. Terrestrial  
488 Remote Sensing of Snowmelt in a Diverse High-Arctic Tundra Environment Using Time-  
489 Lapse Imagery. *Remote Sensing*, 9(7), 1-22. doi: 10.3390/rs9070733.
- 490 Lehejček, J., Buras, A., Svoboda, M., Wilmking, M. (2017) Wood anatomy of *Juniperus*  
491 *communis*: a promising proxy for palaeoclimate reconstructions in the Arctic. *Polar Biol.*,  
492 40,977–988. doi: 10.1007/s00300-016-2021-z.
- 493 Liu, J., Wu, D., Xu, X., Ji, M., Chen, Q., Wang, X. (2021), Projection of extreme precipitation  
494 induced by Arctic amplification over the Northern Hemisphere. *Environ. Res. Lett.* 16 (7),  
495 074012. doi: 10.1088/1748-9326/ac0acc.
- 496 Łupikasza, E. (2007), Wieloletnia zmienność występowania ekstremów opadowych w  
497 Hornsundzie (Spitsbergen) i ich związek z cyrkulacją atmosfery (eng. summary: Long-  
498 term variability of extreme precipitation in Hornsund and its relations to atmospheric  
499 circulation), *Problemy Klimatologii Polarnej*, 17, 87-103. ISSN: 1234-0715.
- 500 Łupikasza, E. (2013), Atmospheric precipitation [in:] Marsz, A. A. & Styszynska, A. (eds).  
501 *Climate and Climate Change at Hornsund, Svalbard*. The publishing house of Gdynia  
502 Maritime University, Gdynia, 199-209. ISBN: 978-83-7421-191-8.
- 503 Łupikasza, E., Niedźwiedź, T. (2019), The Influence of Mesoscale Atmospheric Circulation on  
504 Spitsbergen Air Temperature in Periods of Arctic Warming and Cooling. *Journal of*  
505 *Geophysical Research - Atmospheres*, 124(10), 5233-5250. doi: 10.1029/2018JD029443.
- 506 Łupikasza, E.B., Ignatiuk, D., Grabiec, M., Cielecka-Nowak, K., Laska, M., Jania, J. et al.  
507 (2019), The Role of Winter Rain in the Glacial System on Svalbard. *Water* 11 (2). doi:  
508 10.3390/w11020334.
- 509 Myers-Smith, I.H., Kerby, J.T., Phoenix, G.K., Bjerke, J.W., Epstein, H.E., Assmann, J.J. et al.  
510 (2020), Complexity revealed in the greening of the Arctic. *Nat. Clim. Chang.*, 10, 106-117.  
511 doi: 10.1038/s41558-019-0688-1.
- 512 Niedźwiedź T. (2013), The atmospheric circulation, (in:) Marsz, A. A. & Styszynska, A. eds.  
513 *Climate and climate change at Hornsund, Svalbard*. The publishing house of Gdynia  
514 Maritime University, 57-74. ISBN 978-83-7421-191-8.
- 515 Niedźwiedź, T. (2020), Kalendarz typów cyrkulacji atmosfery dla Spitsbergenu — zbiór  
516 komputerowy, Uniwersytet Śląski, Katedra Klimatologii, Sosnowiec.
- 517 Noël, B., Jakobs, C.L., van Pelt, W.J.J., Lhermitte, S., Wouters, B., Kohler, J. et al. (2020), Low  
518 elevation of Svalbard glaciers drives high mass loss variability. *Nature Communications*,  
519 11(1), 4597. doi:10.1038/s41467-020-18356-1.
- 520 Núñez, J., Rivera, D., Oyarzún, R., Arumí, J.L. (2014), On the use of Standardized Drought Indices  
521 under decadal climate variability: Critical assessment and drought policy implications. *J.*  
522 *Hydrol.*, 517: 458–480. doi: 10.1016/j.jhydrol.2014.05.038.
- 523 Opała-Owczarek, M., Pirożnikow, E., Owczarek, P., Szymański, W., Luks, B., Kępski, D. et al.  
524 (2018), The influence of abiotic factors on the growth of two vascular plant species  
525 (*Saxifraga oppositifolia* and *Salix polaris*) in the High Arctic. *Catena*, 163, 219-232, doi:  
526 10.1016/j.catena.2017.12.018.
- 527 Overland, J.E. (2020), Less climatic resilience in the Arctic. *Weather and Climate Extremes*, 30,  
528 100275. doi: 10.1016/j.wace.2020.100275.

- 529 Owczarek, P., Opała, M. (2016,) Dendrochronology and Extreme Pointer Years in the Tree-Ring  
530 Record (Ad 1951-2011) of Polar Willow from Southwestern Spitsbergen (Svalbard,  
531 Norway). *Geochronometria*, 43(1), 84–95. doi: 10.1515/geochr-2015-0035.
- 532 Owczarek, P., Latocha, A., Wistuba, M., Malik, I. (2013), Reconstruction of modern debris flow  
533 activity in the arctic environment with the use of dwarf shrubs (south-western Spitsbergen)  
534 - a new dendrochronological approach. *Z. Geomorphol. Suppl. Issues*, 57(3), 75-95.  
535 doi:10.1127/0372-8854/2013/S-00145.
- 536 Owczarek, P., Opała-Owczarek, M., Migąła, K. (2021), Post-1980s shift in the sensitivity of tundra  
537 vegetation to climate revealed by the first dendrochronological record from Bear Island  
538 (Bjørnøya), western Barents Sea. *Environ. Res. Lett.*, 16, 014031. doi:10.1088/1748-  
539 9326/abd063.
- 540 Phoenix, G.K., Bjerke, J.W. (2016), Arctic browning: extreme events and trends reversing arctic  
541 greening, *Glob. Chang. Biol.*, 22, 2960-2962. doi: 10.1111/gcb.13261.
- 542 Phulara M., Opała-Owczarek, M., Owczarek, P. (2022), Climatic Signals on Growth Ring  
543 Variation in *Salix herbacea*: Comparing Two Contrasting Sites in Iceland. *Atmosphere*, 13,  
544 718. doi:10.3390/atmos13050718.
- 545 Pithan, F., Mauritsen, T. (2014), Arctic amplification dominated by temperature feedbacks in  
546 contemporary climate models. *Nature Geoscience*, 7, 181-184. doi: 10.1038/NGEO2071.
- 547 Przybylak, R. (2002), Variability of air temperature and atmospheric precipitation in the Arctic.  
548 *Atmospheric and Oceanographic Sciences Library*, Vol. 25. Kluwer Academic Publishers:  
549 Dordrecht. Netherland; Boston. MA; London.
- 550 Przybylak R. (2003), The climate of the Arctic. *Atmospheric and Oceanographic Sciences*  
551 *Library*, Vol. 26. Kluwer Academic Publishers: Dordrecht. Netherland; Boston. MA;  
552 London.
- 553 Reichle, L.M., Epstein, H.E., Bhatt U.S., Raynolds M.K., Walker D.A. (2018), Spatial  
554 heterogeneity of the temporal dynamics of arctic tundra vegetation. *Geophysical Research*  
555 *Letters*, 45, 9206–9215. doi: 10.1029/2018GL078820.
- 556 Rennert, K. J., G. Roe, J., Putkonen, Bitz, C.M. (2009). Soil Thermal and Ecological Impacts of  
557 Rain on Snow Events in the Circumpolar Arctic. *J. of Climate*, 22(9), 2302–2315.  
558 doi: 10.1175/2008JCLI2117.1.
- 559 Reusen, J; Linden, E.D., and Bintanja, R. (2019), Differences between Arctic Interannual and  
560 Decadal Variability across Climate States. *J. of Climate*, 32(18): 6035-6050. doi:  
561 10.1175/JCLI-D-18-0672.1.
- 562 Rouyet, L., Karjalainen, O., Niittynen, P., Aalto, J., Luoto, M., Lauknes, T. R. et al. (2021),  
563 Environmental controls of InSAR-based periglacial ground dynamics in a sub-arctic  
564 landscape. *Journal of Geophysical Research: Earth Surface*, 126, e2021JF006175. doi:  
565 10.1029/2021JF006175.
- 566 Schaefer, K., Lantuit, H., Romanovsky, V., Schuur, E., Witt, R. (2014), The impact of the  
567 permafrost carbon feedback on global climate. *Environ. Res. Lett.* 9, 085003. doi:  
568 10.1088/1748-9326/9/8/085003.
- 569 Schuler, T.V., Kohler, J., Elagina, N., Hagen, J.O.M., Hodson, A.J., Jania, J.A. et al. (2020),  
570 Reconciling Svalbard Glacier Mass Balance. *Front. Earth Sci.*, 8, 1-16. doi:  
571 10.3389/feart.2020.00156.
- 572 Serreze, M.C., Crawford, A.D., Barrett, A.P. (2015), Extreme daily precipitation events at  
573 Spitsbergen, an Arctic island. *Int. J. Climatol.* 35(15), 4574–4588. doi: 10.1002/joc.4308.

- 574 Skagseth, Ø., Furevik, T., Ingvaldsen, R., Loeng, H., Mork, K.A., Orvik K.A. et al. (2008), Volume  
 575 and heat transports to the Arctic Ocean via the Norwegian and Barents Seas. [In:] B.  
 576 Dickson, J. Meincke and P. Rhines (eds), *Arctic–subarctic ocean fluxes: defining the role*  
 577 *of the northern seas in climate*. Springer, Netherlands, 45–64.
- 578 Smith, M.D. (2011), An ecological perspective on extreme climatic events: a synthetic definition  
 579 and framework to guide future research, *J. Ecol.*, 99(3), 656–663. doi: 10.1111/j.1365-  
 580 2745.2011.01798.x.
- 581 Stagge, J.H., Tallaksen, L.M., Gudmundsson, L., Van Loon, A.F., Stahl, K. (2015), Candidate  
 582 Distributions for Climatological Drought Indices (SPI and SPEI). *Int. J. Climatol.*, 35(13),  
 583 4027–4040. doi: 10.1002/joc.4267.
- 584 Strand, S.M., Christiansen, H.H., Johansson M., Åkerman, J., Humlum, O. (2021), Active layer  
 585 thickening and controls on interannual variability in the Nordic Arctic compared to the  
 586 circum-Arctic. *Permafrost and Periglacial Research*, 32, 47-58. doi: 10.1002/ppp.2088.
- 587 van Pelt, W., Pohjola, V., Pettersson, R., Marchenko, S., Kohler, J., Luks, B. (2019), A long-  
 588 term data set of climatic mass balance, snow conditions, and runoff in Svalbard (1957–  
 589 2018), *The Cryosphere*, 13, 2259–2280. Doi:10.5194/tc-13-2259-2019.
- 590 Vicente-Serrano, S.M., Santiago Beguería, S., López-Moreno, J.I. (2010), A Multiscalar Drought  
 591 Index Sensitive to Global Warming: The Standardized Precipitation Evapotranspiration  
 592 Index. *J. of Climate*, 23(7),1696 -1718. doi: 10.1175/2009JCLI2909.1.
- 593 Walczowski, W., Piechura, J. (2011), Influence of the west Spitsbergen current on the local  
 594 climate. *Int. J. Climatol.* 31(7),1088 -1093. doi:10.1002/joc.2338.
- 595 Walsh, J.E., Ballinger, T.J., Euskirchen, E.S., Hanna, E., Mard, J., Overland, J.E. et al. (2020),  
 596 Extreme weather and climate events in northern areas: A review. *Earth – Science*  
 597 *Reviews*, 209, 103324. doi: 10.1016/j.earscirev.2020.103324.
- 598 Wawrzyniak, T., Osuch M. (2019), A consistent High Arctic climatological dataset (1979-2018)  
 599 of the Polish Polar Station Hornsund (SW Spitsbergen, Svalbard). *Pangea*,  
 600 doi:10.1594/PANGAEA.909042.
- 601 Wawrzyniak, T., Osuch, M. 2020. A 40-year High Arctic climatological dataset of the Polish  
 602 Polar Station Hornsund (SW Spitsbergen, Svalbard). *Earth Syst. Sci. Data*, 12, 805–815.  
 603 doi:10.5194/essd-12-805-2020.
- 604 World Meteorological Organization (WMO) and Global Water Partnership (GWP), 2016.  
 605 Handbook of Drought Indicators and Indices (M. Svoboda and B.A. Fuchs). *Integrated*  
 606 *Drought Management Programme (IDMP), Integrated Drought Management Tools and*  
 607 *Guidelines*, Series 2. Geneva.
- 608 Zeng, Z., Li, Y., Wu, W., Zhou, Y., Wang, X., Huang, H. et al. (2020), Spatio-Temporal Variation  
 609 of Drought within the Vegetation Growing Season in North Hemisphere (1982–2015).  
 610 *Water*, 12, 2146. doi:10.3390/w12082146.
- 611 Zhang, K., Kimball, J.S., McDonald, K.C., Cassano, J.J., Running, S.W. (2007), Impacts of large-  
 612 scale oscillations on pan-Arctic terrestrial net primary production. *Geophysical Research*  
 613 *Letters* 34(21). doi:10.1029/2007GL031605.